76th International Astronautical Congress (IAC 2025), Sydney, Australia, 29 Sep-3 Oct 2025.

IAC-25-C3.2.11 (x101967)

Innovative Conceptual Study of an Ultra-Lightweight, Large-Scale Solar Array for Lunar-Orbiting SPS

Yuta Katsuyama[a]*, Ryuya Kumagai[a], Yumi Kawai[a], Takumi Horibe[a], Tomu Matsutomo[b], Naoki Warigai[b], Shinnosuke Sano[c], Yamato Nishida[d], Simon Maillot[e], and Koji Tanaka[f]

[a] *Graduate School of Science and Engineering, Department of Mechanical Engineering, HOSEI University, Kajinocho 3-7-2, Koganei-shi, Tokyo, 184-8584, Japan, yuta.katsuyama.7p@stu.hosei.ac.jp, ryuya.kumagai.9u@stu.hosei.ac.jp. yumi.kawai.7m@stu.hosei.ac.jp, takumi.horibe.6i@stu.hosei.ac.jp.*

[b] *Graduate School of Mechanical and Electrical Engineering, Suwa Tokyo University of Science, 5000-1 Toyohira, Chinoshi, Nagano 391-0292, Japan, gh24532@ed.sus.ac.jp, gh24525@ed.sus.ac.jp,*

[c] *Department of Mechanical Engineering, Faculty of Science and Engineering, HOSEI University, Kajino-cho 3-7-2, Koganei-shi, Tokyo, 184-8584, Japan, shinnosuke.sano.5g@stu.hosei.ac.jp.*

[d] *Department of Mechanical and Electrical Engineering, Suwa Tokyo University of Science, 5000-1 Toyohira, Chinoshi, Nagano 391-0292, Japan, t222351@ed.sus.ac.jp.*

[e] *The Graduate University for Advanced Studies, SOKENDAI, 3-1-1 Yuno-dai, Chuo-ku, Sagamihara-shi, Kanagawa 252-5210, Japan, simon.maillot@ipsa.fr.*

[f] *ISAS/JAXA, Japan, tanaka.koji@jaxa.jp.*

* Corresponding Author

Abstract

In this project, a power generation system for a Lunar-Orbiting SPS was investigated, focusing on lightweight design and improved stowage efficiency to enable construction with a single launch. CIGS thin-film solar cells were adopted, and the target specific power of the system was set to 500 W/kg. Thermal analysis was conducted to estimate the system scale. Increasing the distribution voltage reduced the cable mass, contributing to the achievement of the specific power target and significantly lowering transportation costs. For stowage, Panel fold and Miura fold were compared, and Miura fold was selected as the more effective approach in terms of stowage efficiency and deployment reliability. In addition, risks associated with high-voltage operation, such as discharge and debris impacts, were examined, and these risks can be mitigated through protective coatings and optimized wiring configurations. These results demonstrate the conceptual feasibility of the proposed system.

Keywords: SPS, Lunar, Lightweight, Solar Array, Deployment

Nomenclature

E : Power generation per unit area
T : Temperature of the solar cell
P : Power Output
l : length of one side of the solar array
ρ : Density
R : Resistivity
L : Cable Length
V : Voltage
α : Specific Power
m_s : mass of Solar Cell
m_p : mass of Polyimide Film
m_c : mass of Power Collection and Distribution Cable

Acronyms/Abbreviations

SPS : Solar Power Satellite
PSR : Permanently Shadowed Regions
DC : Direct Current
RF : Radio Frequency
JAXA : Japan Aerospace Exploration Agency

1. Introduction

In recent years, humanity has been advancing into space and expanding its activities with the goal of exploring the Moon, Mars, and beyond. In this context, the United States proposed the Artemis program in 2017, and Japan decided to participate in this program in 2019. As part of the Artemis program, Japan has been conducting research on lunar energy systems necessary for human activities on the Moon.

Water resources have been observed in the regolith of the lunar polar regions, such as the South Pole and Permanently Shadowed Regions (PSR). The areas containing water resources on the Moon's surface are shown in Figure 1. These water resources are crucial for enabling sustainable lunar activities independent of Earth's resources. To make lunar activities sustainable, it is essential to efficiently utilize these water resources. Specifically, water can be extracted on the lunar surface and then converted into hydrogen and oxygen through electrolysis. Through this process, the water resources can be used for the following purposes: First, the converted water can be used as drinking water.

Furthermore, the oxygen generated by electrolysis can be used not only as breathable oxygen for lunar inhabitants but also as a debris shield for spacecraft. Additionally, by combining hydrogen and oxygen, rocket fuel can be supplied for lunar landing and takeoff vehicles.

Solar power is one method of providing energy for human activities on the lunar surface; however, it faces two major challenges. The first challenge is the long duration of the lunar night. On the Moon, approximately 14 days out of the 28-day cycle are in darkness, during which no sunlight is available, making stable power generation difficult. Therefore, it is essential to develop a system that can provide continuous energy supply over extended periods. The second challenge is the presence of PSR. Especially near the lunar south pole, the terrain prevents sunlight from reaching certain areas, making it difficult to generate solar power locally. As a result, systems capable of transmitting energy directly are required.

Currently, the use of a Lunar-Orbiting SPS is considered one of the potential methods for supplying energy to the lunar polar regions. A Lunar-Orbiting SPS is a satellite that converts power generated in lunar orbit into radio waves, millimeter waves, or laser light, and transmits it to any location on the lunar surface. There are two main advantages. The first advantage is its ability to continuously supply power regardless of day or night. The second advantage is the flexibility in selecting the target for power transmission, which is determined by the arrangement of receiving antennas. This allows for the supply of power to a variety of activity locations. Currently, efforts are underway to launch multiple satellites and achieve continuous power transmission through a constellation.

An example of an Earth-Orbiting SPS, known as SPS2000, shows that the power generation system can account for approximately 25% of the total satellite mass. Such a large mass contributes to increased launch costs. In this context, the power generation system refers to the entire satellite system responsible for generating, converting, and delivering electrical power, including solar cells, support films, power collection and distribution cables.

This study focuses on reducing the mass and improving the stowage efficiency of the power generation system for a Lunar-Orbiting SPS. The objective of this study is to enable construction with a single launch and reduce transportation costs to lunar orbit. This research was conducted from the following perspectives:

1. Overview of the traditional tethered SPS for Earth
2. Proposal for a Lunar-Orbiting SPS
3. Consideration of an Ultra-Lightweight Solar Array
4. Examination of Deployment Methods
5. Clarification of challenges

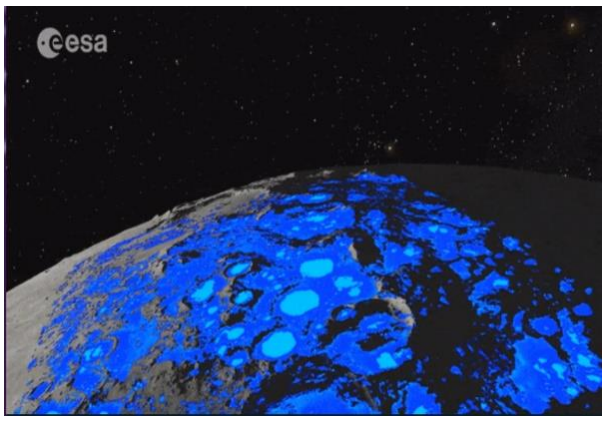

Fig. 1. Regions of water resources on the lunar surface

2. The traditional tethered SPS for Earth

Since Peter E. Glaser first proposed the concept of the Solar Power Satellite (SPS) in 1968, it has been studied by many countries, leading to the consideration of various models.

An overview of the tethered SPS currently being studied in Japan is shown in Figure 2. This system consists of components such as the tether, power generation/transmission panels, and the bus module. By employing a tether with a length of 5 to 10 km, the system can passively maintain a stable Earth-pointing attitude without the need for active attitude control. Solar cells are installed on both surfaces of the power generation/transmission panels, and a power transmission antenna is mounted on the surface facing the Earth. Inside the panel, devices equipped with microwave amplification and power control functions are installed, enabling both power generation and transmission to be carried out on the same panel. The system has a size of approximately 2.5 km on each side and transmits power using microwaves in the 5.8 GHz band.

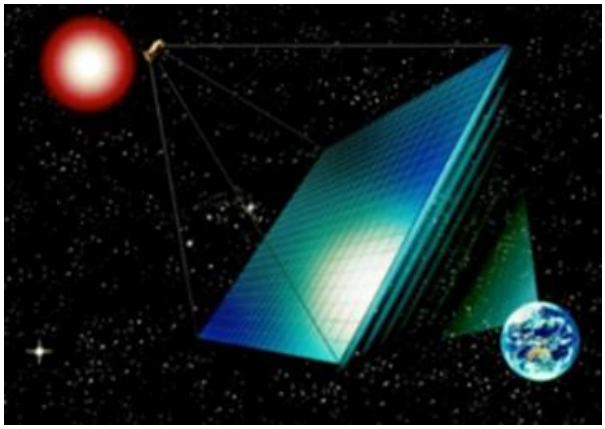

Fig. 2. Illustration of tethered SPS

3. Proposed Lunar Orbiting SPS model

A conceptual drawing of the Lunar-Orbiting SPS is shown in Figure 3. The Lunar-Orbiting SPS differs from the previously described tethered SPS in several ways. First, a configuration in which the power generation system and the power transmission system are separated, rather than integrated power generation/transmission panels, is being considered.

A block diagram of the system configuration is shown in Figure 4. The system consists of two main segments: the orbital segment and the lunar surface segment. The orbital segment includes a large-scale power generation system using solar arrays, a power conversion system that converts DC into RF power, and a RF transmission system deployed in lunar orbit. The lunar surface segment consists of many rectennas, each combining an antenna and a rectifying circuit.

Moreover, since the Moon has no atmosphere, there is no need to consider transmission losses due to atmospheric absorption or scattering of electromagnetic waves. For this reason, although microwave and laser-based wireless power transmission methods have been actively developed for tethered SPS, millimetre-wave transmission is considered a promising option for the Lunar-Orbiting SPS as well.

The specifications of the Lunar-Orbiting SPS are shown in Table 1.

Table 1 Specifications of the Lunar-Orbiting SPS

Orbit	Apoapsis: 1000km Periapsis: 100km
Power generation	200 kW
Number of Satellite	5 units
Supply Power	136.3 kW
Frequency	5.758 GHz

The orbit is set to a highly elliptical orbit, passing over the lunar south pole, with an apolune altitude of 1000 km and a perilune altitude of 100 km. For water resource exploration activities on the lunar surface, approximately 100 kW of electric power is assumed necessary. Therefore, to achieve continuous power transmission of approximately 100 kW through constellation operation, a generated power of 200 kW is necessary.

The system employs a constellation of five satellites. As a result, the transmission power required per satellite for continuous power delivery is 136.3 kW. The transmission frequency is set to 5.758 GHz.

The total mass of the bus and transmission sections per satellite, estimated from the above parameters, is approximately 20–25 tons, with about 10–15 tons for the bus section and about 10 tons for the transmission section.

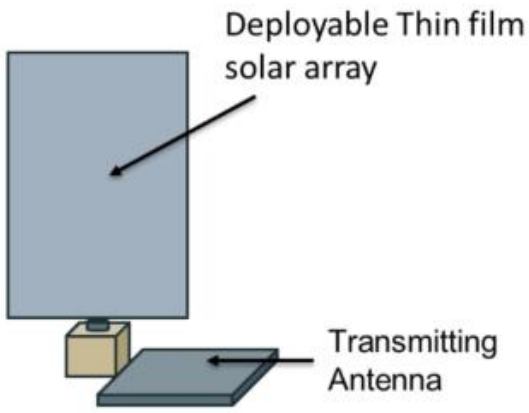

Fig. 3. Conceptual drawing of the Lunar-Orbiting SPS

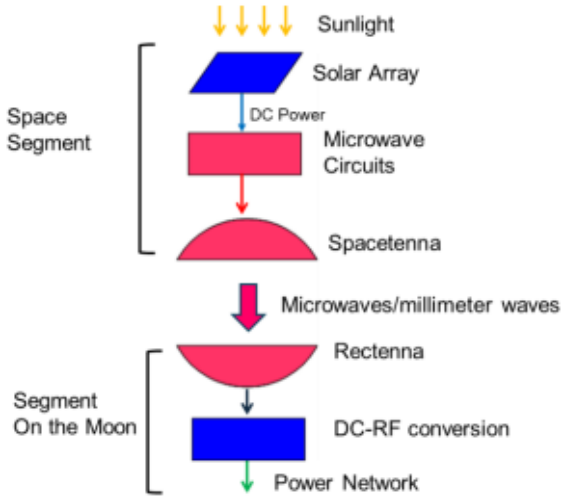

Fig. 4. Block Diagram of the Lunar-Orbiting SPS

4. Consideration of Ultra-Lightweight Solar Array

4.1 Selection of Thin-Film Solar Cells

As an example of conventional power generation systems, the solar arrays of the ISS can be cited, with a specific power limited to about 30 W/kg. To achieve higher specific power, significant weight reduction of the power generation system is required, thus making thin-film solar cells, which are lightweight, flexible, and foldable, indispensable.

Among thin-film solar cells, CIGS and 3J-GaAs have been widely recognized for their potential in space applications and were selected as representative candidates in this study.

CIGS (Copper Indium Gallium Selenide) is a compound semiconductor-based solar cell composed mainly of four elements: copper, indium, gallium, and selenium. CIGS offers high reliability over the long term due to its low degradation over time, and it also exhibits

excellent radiation resistance, making it suitable for use in space environments.

3J-GaAs is a triple-junction solar cell composed of stacked compound semiconductors such as Indium Gallium Phosphide (InGaP), Gallium Arsenide (GaAs), and Indium Gallium Arsenide (InGaAs). Its main feature is a high-power conversion efficiency of approximately 30%.

The mass characteristics of CIGS and 3J-GaAs were compared. The results are shown in Figure 5. The specific power of CIGS is 922 W/kg, which significantly exceeds that of 3J-GaAs. Based on this, CIGS was selected for this project due to its higher specific power.

The power generation system consists of solar cells, support films, power collection and distribution cables. Considering their masses, the target specific power of the lunar-orbiting SPS power generation system in this project is set to 500 W/kg.

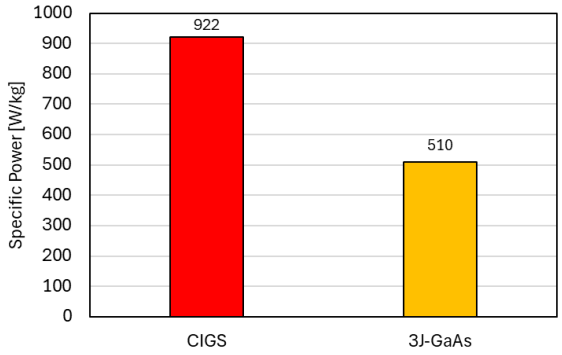

Fig. 5. Specific Power of CIGS and 3J-GaAs

4.2 Thermal Analysis

Solar cells exhibit a temperature dependence in which their power generation efficiency decreases as the surface temperature rises.

For CIGS solar cells (Ascent SOLAR), experiments have shown that when the temperature varies from 40 °C to 120 °C, the power output per unit area can be expressed by the following equation.

$$E = -0.5055T + 126.97 \qquad (1)$$

In this study, the temperature of the solar array during the lunar polar orbit of the Lunar-Orbiting SPS is investigated, and based on the results, the required area of the solar array is calculated to determine the system size.

In the thermal analysis, Patran (pre/post-processing) and Nastran (solver) were used to perform the temperature analysis. For the analysis, solar radiation was considered as the thermal input in the lunar polar orbital environment. Because thermal exchange in space occurs primarily through radiation, the absorptivity and emissivity of the solar array surface were specified, and under these conditions, a temperature variation simulation over three orbital cycles was conducted. The simplified model of the solar array, excluding cables and other auxiliary components, is shown in Figure 6.

In this analysis, the model was oriented toward the Sun, and the thermal input was set to solar radiation of 1,367 W/m². For the orbital conditions, a simulation was conducted with an orbital period of 9,895 seconds per cycle. The material properties of the structural components are shown in Table 2.

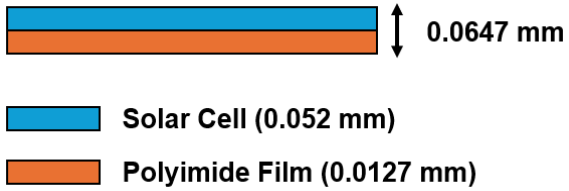

Fig. 6. The structure of the Solar Array

Table 2 Material Properties

Material	Polyimide Film	Solar Cell
Thermal Conductivity [W/m·K]	0.16	8.00
Specific heat capacity [J/kg·K]	1100	1.13
Density [kg/m^3]	1420	2002
Emissivity	0.55	0.53
Absorptivity	0.34	0.87

4.3 Determination of Solar Array Size

According to Equation (1), the power generation per unit area of the solar cell decreases as its surface temperature increases. Therefore, by calculating the required panel area based on the power output at the equilibrium temperature, a conservative design can be achieved.

The analysis results showed that the equilibrium temperature of the solar cell was found to be 100.45 °C. Based on this result, the size of the solar cell panel was calculated using the following equation, assuming that the panel is square.

$$l = \sqrt{\frac{P}{E}} \qquad (2)$$

As a result of the calculation, it was found that each side of the solar array needs to be 51.23 m in length.

4.4 Estimation of mass of Power Collection and Distribution Cables

The power collection and distribution cables are used to aggregate the generated power and deliver it to the transmission system. In this project, it is assumed that the cables are arranged across the solar panels, spaced at 2 m intervals.

The mass of the cable was calculated based on the size of the solar cell array.

The voltage varied from 100 V up to 700 V, with the reduction rate reaching approximately 15%. The calculation formula for the power collection and distribution cables is shown below.

$$m_c = \frac{0.9P\rho RL^2}{V^2} \qquad (3)$$

The values used in the calculations are presented in Table 3, and the calculation results are shown in Figure 7.

The cable mass decreased significantly in the range of 100 to 300 V, while the rate of decrease decreased at a slower rate above 300 V.

Table 3 Parameters for Cable Mass Calculation

Item	Symbol	Value
Supplied Power [W]	P	200000
Resistivity [Ω·m]	R	2.65×10^{-8}
Density [kg/m^3]	ρ	2700
Side length [m]	l	51.23
Side length [m]	L	1200

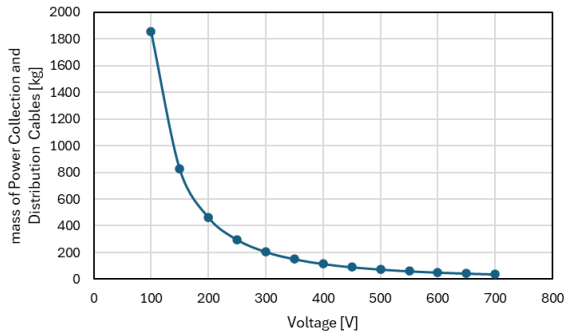

Fig. 7. mass of Power Collection and Distribution Cable

4.5 Estimation of Specific Power of Solar Array

The mass of the polyimide film and solar cell was calculated based on the size of the solar array. These results are shown in Table 4.

Table 4 mass of Polyimide Film and Solar Cell

	Polyimide Film	Solar Cell
mass [kg]	47.34	273.28

The specific power of the solar array was calculated from Table 4 and Figure 7 using the following equation, and the results are shown in Figure 8.

From Figure 8, it was found that the required voltage to achieve the target of 500 W/kg was 484V.

$$\alpha = \frac{P}{m_s + m_p + m_c} \qquad (4)$$

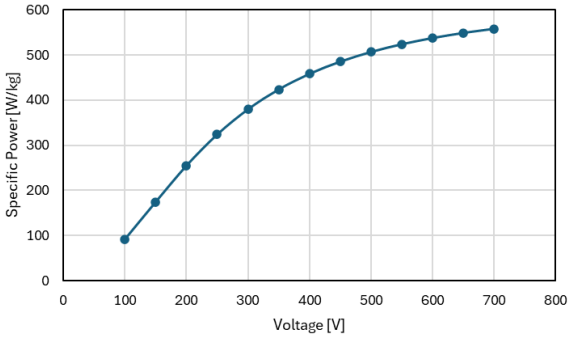

Fig. 8. Specific Power of Solar Array

4.6 Estimation of Transportation Cost Savings

A comparison was made between the transportation cost of the power generation system using current technology (120 V), transported by Starship (SpaceX), and that of the system studied in this project (484 V). The cost reduction achieved through weight savings was calculated, and the results are shown in Table 5. The transportation cost to lunar orbit is estimated to be $1000/kg after 2030.

Table 5 Transportation Cost Savings from Lightweight

Voltage	120 V	484 V
mass of Solar Array [kg]	1608.51	399.78
Transportation Cost [$]	1,608,513	399,782

The use of a higher voltage is estimated to reduce launch costs by $1,208,731.

5. Examination of Deployment Methods

In the construction of a Lunar-Orbiting SPS, the stowage efficiency of the power generation system is a critical factor affecting both launch costs and system reliability. This study compares two representative methods: Panel fold (Figure 9) and Miura fold (Figure 10). For a 20 m × 20 m thin film, the stowage efficiency of each fold method was evaluated, and the number of panels that can be accommodated on a Starship was calculated.

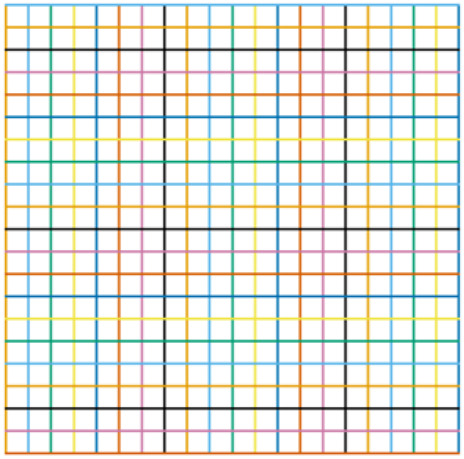

Fig. 9. Crease pattern of Panel fold

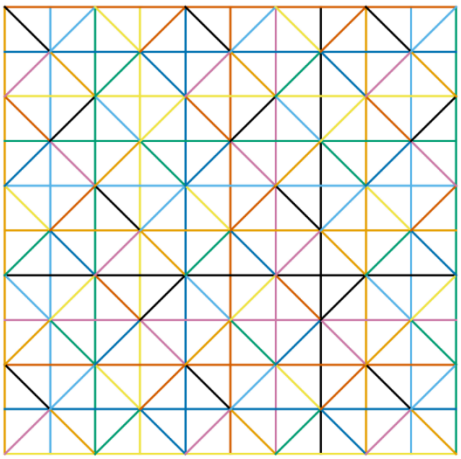

Fig. 10. Crease pattern of Miura fold

5.1 Comparison of Stowage Efficiency between Miura fold and Panel fold

The target membrane was assumed to have a thickness of 1 mm, an area of 400 m², and a volume of 0.400 m³. In the case of Miura fold, the membrane was processed into strips, and the required height was calculated when stowed on a roll with an outer diameter of 1.0 m and a core diameter of 0.3 m. For Panel fold, the membrane was divided into square panels of 2.0 m, 1.0 m, and 0.5 m, and the stacking thickness when laid flat was calculated. The results are shown in Figure 11. The stowage height for the Miura fold roll was approximately 0.56 m. The stacking thickness for Panel fold was 0.10 m for 2.0 m panels, 0.40 m for 1.0 m panels, and 1.60 m for 0.5 m panels. Although Panel fold shows high stowage efficiency under ideal conditions, additional elements such as fixtures, deployment mechanisms, and impact protection are likely to reduce the actual efficiency. On the other hand, while Miura fold slightly increases its thickness, it offers superior deployment reliability and operability, providing significant advantages in actual operations.

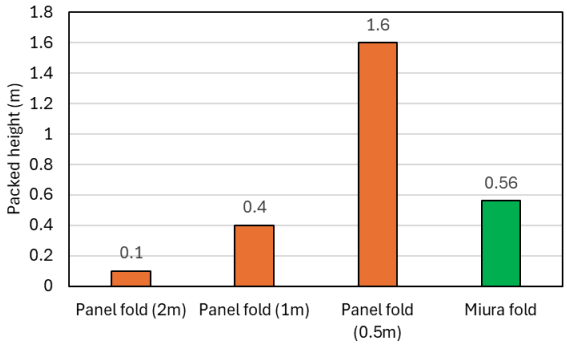

Fig. 11. Comparison of packed heights

5.2 Comparison of the Number of Panels That Can Be Accommodated on a Starship

Assuming the Starship payload bay as a cylinder with a diameter of 9.0 m and a height of 18.0 m, the effective volume was estimated to be approximately 1,145 m³. Under this assumption, the number of panels that can be accommodated was calculated based on Miura fold roll stowage and 1 m × 1 m panel stacking.

In the case of Miura fold, when stowed on a roll with an outer diameter of 1.0 m and a core diameter of 0.3 m, the required height per membrane is approximately 0.56 m. The roll occupies about 0.785 m² on the payload floor, allowing an ideal arrangement of 81 rolls on the floor. Furthermore, 32 layers of rolls can be stacked in a vertical direction, resulting in a total of 2,592.

On the other hand, when the membrane is divided into 1 m × 1 m panels, each membrane consists of 400 panels. Assuming the panels are 1 mm thick and lay flat on the floor, approximately 63 panels can be arranged per layer, and theoretically, 18,000 layers can be stacked within the 18 m height, giving a total of about 1,145,000 panels. Converting this back to membranes, the number of membranes that can be accommodated is approximately 2,862.

These results indicate that the panel stacking method achieves slightly higher volumetric efficiency, accommodating about 10% more membranes than the Miura fold roll. However, the roll stowage method offers higher deployment reliability, whereas the panel stacking method requires more complex fixtures and deployment mechanisms. Considering these trade-offs, Miura fold was selected for this study. It should be noted that these calculations are based on ideal packing assumptions. In practice, structural fixtures, clearances to prevent interference, and vibration isolation mechanisms will reduce the effective packing density. Therefore, the actual number of membranes that can be stowed will be

smaller than the theoretical maximum. Under such practical conditions, Miura fold is expected to provide superior stowage performance due to its simpler fixture requirements and higher deployment reliability.

6. Future Challenges

6.1 Necessity of thermal design of Solar Array

In this study, a thermal analysis was conducted to determine the system size based on the equilibrium temperature of the solar cell surface. The operational temperature range of the solar cells is specified as −140 ℃ to 125 ℃. The analysis results indicated that, although the equilibrium temperature remained within this range, the minimum temperature during lunar eclipse reached −216.59 ℃, which exceeds the lower operational limit. Countermeasures considered include the application of multilayer insulation, surface treatments such as low-emissivity coatings, and the incorporation of planar heaters. While these measures inevitably increase the system mass and consequently introduce a trade-off with the specific power, the issue of extremely low temperature is critical and must be addressed to ensure the viability of the proposed system.

6.2 Challenges associated with high-voltage operation

The maximum voltage currently used in spacecraft is the 120 V DC system of the ISS. However, when operating a 100 kW-class SPS in lunar orbit, a 120 V system would result in excessive wiring mass and transmission losses, making high-voltage operation essential. The adoption of high voltage introduces several electrical risks in solar arrays composed of CIGS thin-film solar cells, polyimide film substrates, and power collection and distribution cables.

First, degradation of the cells due to transient discharges is a concern. When the satellite surface becomes charged by plasma in the solar wind, local discharges can repeatedly occur at triple-junction interfaces, such as the CIGS cells, polyimide film, and vacuum interface, potentially reducing cell performance. To mitigate this, applying a protective layer to the thin film can effectively suppress the occurrence of discharges.

In addition, collisions with space debris also increase the risk of discharges. High-velocity impacts can generate localized high-voltage plasma, causing short circuits between cells and power collection and distribution cables, which may lead to sustained discharges. To address this, a series-parallel wiring configuration, rather than a simple series connection, can be employed to ensure that the overall system continues to operate even if some elements are damaged.

In summary, through structural and material design measures, the high-voltage discharge risk in this type of solar array can be expected to be mitigated.

6.3 Challenges of Miura fold

While Miura fold offers high reliability for the simultaneous deployment of large-area membranes, a challenge arises when applying it to actual solar panels due to reduced packing efficiency. Specifically, constraints imposed by the crease pattern and deployment mechanism make it difficult to uniformly lay solar cells across the entire membrane, resulting in a lower cell placement density. Therefore, optimization of panel size and careful design of the crease layout, are crucial for achieving high packing efficiency.

7. Conclusions

In this study, a conceptual design of a power generation system for a Lunar-Orbiting SPS was conducted and demonstrated the potential to achieve a specific power of 500 W/kg using CIGS thin-film solar cells. Thermal analysis indicated that the required panel size is 51.23 m × 51.23 m. By increasing the distribution voltage to 484 V, the mass of the cables was reduced, thereby achieving the target specific power of 500 W/kg. Furthermore, the higher operating voltage could potentially reduce launch costs by approximately USD 1.21 million.

Regarding the deployment mechanism, a comparison between Panel fold and Miura fold was made. Miura fold was adopted due to its high stowage efficiency under practical conditions and superior deployment reliability for large-area membrane structures.

To mitigate risks associated with high-voltage operation, such as discharge and debris impact, measures to improve reliability, including protective coatings and series-parallel wiring configurations, were proposed.

Analysis revealed that in an extremely low-temperature environment during a lunar eclipse, where temperatures of solar cells can drop to −216 °C, the solar cells would exceed their operational limits, indicating the necessity of additional thermal control measures.

Future work includes performing thermal analyses and thermal vacuum tests of solar arrays with thermal countermeasures, as well as analyses of the Miura fold deployment mechanism, to further verify the feasibility of the proposed Lunar-Orbiting SPS.

Acknowledgements

This study is supported by SPACE Canada.

References

[1] Peter. E. Glaser, Power from the Sun: Its future, Science Vol. 162, issue 3856, pp857-861, (1968), American Association for the Advancement of Science

[2] National Aeronautics and Space Administration, "Artemis" https://www.nasa.gov/humans-in-space/artemis/

[3] Kazuyoshi ARAI, Hideaki TAKAHASHI, Shunsuke URASAWA and Sunao HASEGAWA, Ballistic Limit Velocity of Space Debris Shield used Liquid Layer, Aerospace Technology Vol.11, pp. 117-122, 2012 https://doi.org/10.2322/astj.11.117

[4] N. Shinohara, Forest of knowledge, Space solar power, in: IEICE (Ed.), Ohmsha, Ltd., Tokyo, 2012, in Japanese.

[5] Japan Space Systems, Research and Development Roadmap for the 2006 Model of the Integrated Power Generation and Transmission Space Solar Power System, (2017). https://www.jspacesystems.or.jp/jss/wp-content/uploads/2021/07/SSPS_H28_Roadmap_a.pdf

[6] Koji Tanaka, Yoshiyuki Fujino, Kenji Ito, Tomohiko Mitani, Ryu Ishikawa, Kazuhiko Honjo, Kosei Ishimura, Kenji Yamauchi, Koichi Ijichi, Noriaki Oka, Atsushi Uchida, Conceptual study of energy supply from lunar orbit, 35th ISTS Organizing Committee 2025-q-3-5

[7] Sharp's thin-film compound solar cells were used in JAXA's small demonstration spacecraft, "SLIM," which successfully achieved "high-precision landing" on the lunar surface. https://corporate.jp.sharp/news/240129-b.html

[8] EnergyPal Solar Panel Guide Specification Data Sheet, Ascent SOLAR BARE MODULES MINI-SCALE GROUP. https://cdn.energypal.com/panels/b-003-018-026/energypal-solar-panel-spec-datasheet-ascent-solar-technologies-solar-bare-modules-mini-scale-b-003-018-026.pdf

[9] Ministry of Economy, Trade and Industry (METI), FY2022 Supplementary Budget for Space Development and Utilization Promotion Research and Development: Energy-Related Technology Development on the Lunar Surface (Technical Issue Compilation) https://www.meti.go.jp/meti_lib/report/2022FY/060249.pdf

[10] Ministry of Economy, Trade and Industry (METI), FY2024 Supplementary Budget for Space Development and Utilization Promotion Research and Development: Energy-Related Technology Development on the Lunar Surface (Technical Issue Compilation) https://www.meti.go.jp/meti_lib/report/2024FY/10000072.pdf

[11] CHO, Mengu, "High Voltage Solar Array, https://www.jstage.jst.go.jp/article/jvsj2/51/8/51_8_519/_pdf

[12] Ferguson, D. C., Galofaro, J. T., & Vayner, B. V. (2003). New voltage and current thresholds determined for sustained space plasma arcing (NASA Technical Report No. 20050214579). NASA Glenn Research Center. https://ntrs.nasa.gov/api/citations/20050214579/downloads/20050214579.pdf

[13] NASA. (2018). Low Earth Orbit Spacecraft Charging Design Handbook (NASA-HDBK-4006A). https://standards.nasa.gov/sites/default/files/standards/NASA/A/0/nasa-hdbk-4006a.pdf

[14] Toray DuPont Co., Ltd. (2007). Kapton®: High-temperature and low-temperature resistant polyimide film. https://www.tdnet.co.jp/kapton/data/download/documents/kapton2007.pdf

[15] Henninger, J. H. (1984). Solar absorptance and thermal emittance of some common spacecraft thermal-control coatings (NASA Reference Publication 1121). NASA Goddard Space Flight Center. https://ntrs.nasa.gov/api/citations/19840015630/downloads/19840015630.pdf?utm_source=chatgpt.com